ISSN: 2641-192X
DOI: 10.33552/JTSFT.2024.11.000755
Journal of
Textile Science & Fashion Technology
Iris Publishers

Research Article

Synthesis of Schiff Base Photochromic Dyes and Dyeing Properties on Polyester Fabrics

Jiansheng Dong[1], Wenjun Meng[1], Leilei Si[1], Yudong Wang[2]*and Yunjie Yin[1]*

[1]*College of Textile Science and Engineering, Jiangnan University, Wuxi 214122, China*

[2]*College of Biological and Chemical Engineering, Guangxi University of Science & Technology, Liuzhou 545006, China*

***Corresponding author:** Yunjie Yin and Yudong Wang*, College of Textile Science and Engineering, Jiangnan University, Wuxi 214122, China. College of Biological and Chemical Engineering, Guangxi University of Science & Technology, Liuzhou 545006, China

Received Date: November 25, 2024

Published Date: December 09, 2024

Abstract

A novel Schiff base compound, 5-chlorosalicylaldehyde carbonyldihydrazide Schiff base (CSHA), featuring photochromic and fluorescent properties was synthesized from 5-chlorosalicylaldehyde and dihydrazide carbonate. Infrared Radiation (IR) and UV analyses confirmed the chemical structure of CSHA. The compound's thermal stability, discoloration sensitivity, and optimal yield reaction time were evaluated. CSHA nano-disperse dyes were prepared through mortar grinding, ultrasonication, and homogenization, and used to fabricate photochromic polyester fabrics via high-temperature and high-pressure techniques. The dyed fabric exhibits a yellow colour with a maximum chromatic aberration of 19.45, and minimal impact on the fabric's thermal decomposition temperature. Under UV light excitation, the fabric showed a fluorescence emission wavelength of 562 nm and a maximum fluorescence intensity of 5207, alongside excellent UV resistance and colour fastness. This makes CSHA dyes suitable for high-temperature and high-pressure dyeing applications.

Keywords: Schiff base compounds; photochromism; fluorescence properties; direct dyeing; polyester fabric

Introduction

Colour-changing materials that react to their surroundings have garnered considerable interest from scientific and commercial communities. These materials exhibit discernible colour transformations in response to environmental stimuli such as pH, temperature, light exposure, vapour [1], mechanical stress [2,3], or electrical inputs. Through the absorption of light across different spectral ranges, the chemical constituents within photochromic compounds undergo a reversible, light-induced transition between two distinct states [4]. Photochromic systems are broadly categorized into inorganic and organic types [5-7]. The primary constituents of inorganic photochromic systems include alkaline earth metal sulfides, transition metal complexes, and transition metal oxides. Although a diverse array of organic photochromic compounds exists, research predominantly centers on key organic molecules, such as azo benzene [8-11], spiro pyran [12-15], spiro oxazine [16], captive arginine [17-21], diaryl ethylene [22-24], and salicylaldehyde Schiff base [25]. Schiff bases, characterized by their imine structures, are synthesized through the condensation of aldehydes and ketones with amino groups. The imine-containing salicylaldehyde structures of Schiff base compounds can establish hydrogen bonds with the hydroxyl group within the salicylaldehyde moiety. Subject to specific external stimuli, such as heat, light, and near-infrared radiation, these compounds can undergo intramolecular proton transfer, altering the molecular structure

from alcoholic to ketonic, thereby inducing photochromic, thermochromic, and photoluminescent effects. Consequently, Schiff bases and their derivatives find extensive applications in the domains of biological antimicrobial activity, color change induction, functional material development, catalysis, and analytical science. For applications such as textile printing and coating, photochromic materials like spiro-pyran necessitate microencapsulation [26]. Although this technique substantially enhances the fatigue resistance of spiro-pyran materials and mitigates photo-oxidation, it also results in a decelerated color change response time for the encapsulated spiro-pyran. Additionally, the color phase of the spiro-pyran material pre- and post-color transition is affected by the encapsulating shell layer [27].

In the preliminary stages, numerous researchers across various fields have conducted detailed investigations into photochromic materials. These substances are predominantly employed for purposes such as anti-counterfeiting, bio-imaging, optical information storage, and textiles. Upon exposure to light, these materials can undergo significant color transformations. Nevertheless, the color reverts back once the light source is eliminated or when stimulated under particular conditions. Bikash Garai developed a photochromic metal-organic framework (MOF) to serve as a medium for erasable inkless printing, leveraging the reversible color-changing characteristics of photochromic materials. This was accomplished by exposing MOF-coated paper to daylight to mimic the printing process and altering the structure of various MOFs to achieve analogous effects in different colors, thereby enhancing resolution, stability, and fatigue resistance [28]. Similarly, Sameh Helmy synthesized a novel organic photochromic molecule for the creation of visible light-controlled photoswitches DASAs, which exhibit potential applications in biosensor-targeted delivery systems [29]. For the purposes of anti-counterfeiting and achieving high-resolution imaging, Qi has developed a solid-state photo-induced switching material, utilizing a spiro-pyran dimeric anthracene derivative (DSA-2SP). This material, DSA-2SP, demonstrated reversible absorption and emission light modulation capabilities, facilitating an efficient photo-switching mechanism between DSA-2SP and its photoisomer, DSA-2MC [30]. The utilization of Schiff base photochromic materials in textile applications remains relatively uncommon, which presents a promising avenue for the incorporation of these materials into textiles, a subject that will be the focal point of our forthcoming research.

In this investigation, to advance the utilization of photochromic materials on textiles and explore potential application scenarios, we synthesized a Schiff base photochromic material and direct dyes polyester fabrics. A Schiff base compound, 5-chlorosalicylaldehyde carbonyldihydrazide Schiff base (CSHA), embodying both photochromic and fluorescent functionalities, was developed. CSHA is characterized by its typical aggregation-induced emission (AIE) [31] properties, attributable to restricted intramolecular rotations (RIR) and excited-state intramolecular proton transfer (ESIPT) processes [32]. The photochromic molecule CSHA is capable of reversible color and fluorescence changes when upon exposed to UV light, exhibiting commendable fatigue resistance. To scrutinize the reactions involving the Schiff base, an examination of the synthesis duration's influence on CSHA was conducted. Subsequently, the synthesized Schiff base compound was employed to formulate disperse dyes, suitable for the high-temperature and high-pressure dyeing process of polyester. The chemical constitution of CSHA was assessed through IR and UV absorption spectroscopy, affirming its congruence with the hypothesized structure. The sensitivity to color change was evaluated and corroborated alignment with the theoretical expectation. Scanning Electron Microscopy (SEM) facilitated the examination of the microscopic morphology of polyester fabrics dyed with CSHA disperse dyes. Comprehensive analyses of the chromatic aberration, dye absorption, fluorescence characteristics, and color stability of the prepared Schiff base polyester fabrics culminated in the delineation of optimal dye concentration parameters for polyester dyeing.

Material and Methods

Materials and reagents

Dihydrazide carbonate was purchased from Aladdin. The polyester fabric was obtained from Hebei Linlon Textile Co., Ltd. The experimental materials and solvents, such as 5-Chlorosalicylaldehyde with mass concentration ≥98%, Tween 80, and Sodium-4A type Molecular Sieve, were offered from Sinopharm Group Chemical Reagent Co., Ltd.

Preparation of 5-chlorosalicylaldehyde hydrazide Schiff base

Carbonyl hydrazide (4.5 g, 0.5mol) and 5-chlorosalicylaldehyde (3.1 g, 1mol) were synthesized and subjected to reflux at 81 °C in 20 mL of ethanol, following the methodology prescribed in the literature. The extraction of the crude products was completed over a period of two hours. The pure CSHA (83% yield) was obtained by recrystallizing the compound using a mixed solvent system (V (dichloromethane): V (ethanol) = 3:1). The synthesis of compound CSHA is depicted in Figure 1.

Pre-staining preparation

The purified home-made Schiff base photochromic compound was subjected to pulverization in a mortar and subsequently ball-milled with zirconium beads to attain a desire particle size, following which dispersions were formulated in various mass fractions. The polyester fabric was segmented into dimensions of 5 cm by 25 cm, subjected to detergent washing, air-dried, and sequentially numbered from 1 to 5, thereafter being weighed. A dye bath ratio of 1:50 was employed, the quantity of dye was calibrated to correspond to 5%, 10%, 15%, 20%, and 25% of the fabric's mass, based on the weighted mass of each fabric segment, and the concentration of triton dispersant was fixed at 0.2%.

Direct dyeing of polyester fabric with CSHA dyes

In the high-temperature and high-pressure dyeing process, the polyester fabric undergoes dyeing at a heating rate of 2°C/min, followed by a cooling down to 70°C for removal. Compounds

such as Schiff bases and disperse dyes, characterized by their simplistic chemical structures, are capable of forming dispersion systems within the aqueous phase. This characteristic facilitates their integration into polyester fibers under high temperatures and pressures. Nonetheless, to augment the color fastness and gloss of dyed polyester garments, it is imperative that Schiff base compounds undergo a cleansing process with alcohol to eradicate surface compounds failing to permeate the fibers [45]. Subsequent to the dyeing process, the dyed polyester fabric must be immersed in an ethanol aqueous solution with a 30% v/v concentration at a 1:50 bath ratio, subjected to frequent washing to remove any residual dye, thoroughly rinsed with deionized water, and finally, dried.

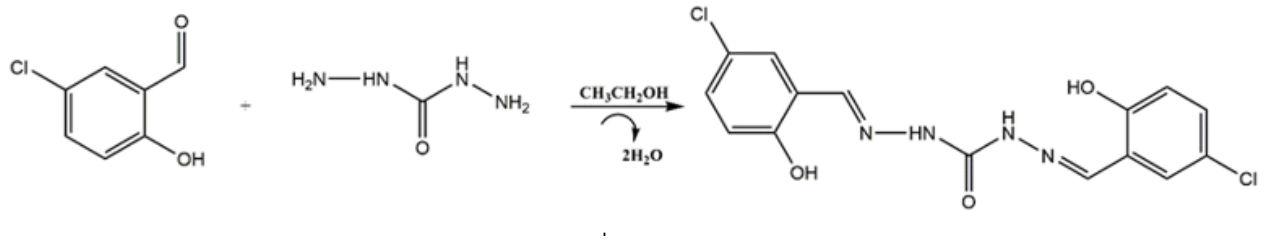

Figure 1: The creation of compound CSHA (yield 83%).

Characterization

The particle size and particle size distribution of Schiff base compounds CSHA were examined using a combination of Zeta potential and a particle size analyzer (Brookhaven, Ltd., American). The structures of the Schiff base compounds CSHA were determined using a NICOLET iS10 transform infrared instrument (Thermo Fisher Scientific, Co. Ltd., China) with KBr disks in the range of 500–4000 cm-1 at a temperature of 25°C. In addition, scanning electron microscopy (SEM) was used to photograph each sample with an SU1510 (Hitachi, Ltd., Japan). The thermal stability of the original polyester fabric and the CSHA photochromic polyester fabric was determined by analyzing a TA-Q500 thermogravimetric analyzer (Suzhou Sato Precision Instruments Co.) in a nitrogen atmosphere at a heating rate of 10°C/min from 30°C to 900°C, followed by a cooling rate of 50°C/min to room temperature. Furthermore, the DSC (differential scanning calorimetry) of Schiff base compounds CSHA was measured from 25°C to 200°C (scanning rate of 10°C/min) using the thermogravimetric analyzer mentioned above under a flow of nitrogen gas. To evaluate the particle size distribution of CSHA disperse dyes, 0.01 g of CSHA disperse dyes dispersion underwent ultrasonic dispersion and was loaded into a test dish. The particle size distribution was then characterized by the log-normal intensity at room temperature (25°C).

The UV absorption spectrum of the sample was tested using a UV spectrophotometer with a wavelength range of 200–400 nm after dissolving 0.001 g of the sample in 10 mL of DMF (N, N-dimethylformamide) solvent. Finally, the fluorescence intensity of the sample fabric was determined using a fluorescence spectrophotometer with an excitation wavelength of 365 nm and a test range of 400–700 nm. The K/S data of the CSHA film were measured before and after exciting the film at 400–700 nm using a computerized colorimeter. The K/S values of the fluorescent printed fabrics were also measured under a D65/10 light source, and the reflectance of the fabrics was evaluated at 0% and 100% UV transmittance of the light. The reflectance of the CSHA photochromic polyester fabric was assessed both before and after the color shift. To evaluate the chromatic aberration and dye uptake of the polyester fabric, color matching was performed using a D65/10 light source. The absorbance A0 and A1 at the maximum absorption wavelength were measured using a spectrophotometer. Polyester fabric dye uptake was determined using the equation: (1-A1/A0) × 100%, where A0 represents the absorbance of the dyeing solution before dyeing and A1 represents the absorbance of the residual solution after dyeing. In addition, the wet and dry rubbing fastnesses of the printed polyester fabric were assessed in accordance with the ISO 105-X12:2001 method. The washing fastness of the printed polyester fabric was evaluated using the SW-12 washing fastness tester, in accordance with the AATCC 61-2007 standard.

Results and Discussion

Infrared spectral analysis

As depicted in Figure 2a, the IR spectra of the precursor materials employed in synthesizing the compounds exhibited a pronounced peak around 3215 cm^{-1}, attributable to the stretching vibration of the connected hydroxyl group (-OH) and the unsaturated C-H stretching vibration within the aldehyde group of the 5-chlorosalicylaldehyde. The absorption at 3046 cm-1 was ascribed to the C-H stretching vibration in the benzene ring. The aldehyde group's carbonyl (C=O) in salicylaldehyde manifested a sharp, intense absorption peak at 1655 cm^{-1}, while the absorption peak at 700 cm^{-1} resulted from the chlorine substitution at the benzene ring's fifth position. In the IR spectra of dihydrazide carbonate, the absorption peaks at 3351 cm^{-1}, 3323 cm^{-1}, 3300 cm^{-1}, and 3194 cm^{-1} were attributed to the free and conjugated primary amine-NH2 and secondary amine-NH within the structure, whereas the absorption

peak at 1630 cm^{-1} represented the characteristic absorption peak of carbonyl-C=O. Similarly, the carbonyl group in the original carbonic dihydrazide shifted from the absorption peak at 1630 cm^{-1} to 1619 cm^{-1}, signifying a modification in the chemical environment surrounding the carbonyl group. Nevertheless, the aldehyde peak in the initial 5-chlorosalicylaldehyde retained its absorption peaks at 3043 cm^{-1} and 3232 cm-1 in comparison to the IR spectra of the precursor materials. The disappearance of the aldehyde peak from the initial 5-chlorosalicylaldehyde, with the emergence of a distinct imino-C=N absorption peak at 1676 cm^{-1}, evidenced the absence of an unreacted amino group in the chemical system. Consequently, it is deduced that the aldehyde and amino groups effectively reacted through a Schiff base reaction to form CSHA.

The Schiff base reaction involving CSHA is characterized by high efficiency and swift completion. Nonetheless, it eventually attains an equilibrium state, precluding further advancement despite prolonged durations. This stagnation, due to economic limitations, is suboptimal for both the synthesis and practical application of CSHA in industrial processes. To pinpoint the most favorable reaction conditions and secure the highest yield within a feasible timeframe, an analysis of differing reaction durations was performed during the reflux of CSHA Schiff base in ethanol. The objective was to determine the ideal reaction duration, thereby enhancing efficiency and reducing the financial burden of extended reaction periods. By identifying the optimal reaction time, our intention was to reconcile high yield with cost-effective production, thereby facilitating the successful implementation of the CSHA Schiff base reaction.

Figure 2b depicts the interaction between 5-chlorosalicylaldehyde and dihydrazide carbonate at a 2:1 feeding ratio. With the prolongation of reaction time, the imino-C=N absorption peak promptly manifested at 1676 cm-1 on the infrared spectrum. The peak's intensity augmented consistently as the reaction time extended, reaching its zenith at 1.5 hours, signifying the completion of the Schiff base reaction at this juncture. The raw material, dihydrazide carbonate, is characterized by the green and brown bands. The persistence of these absorption peaks throughout the reaction process suggests the presence of unreacted dihydrazide carbonate in the system, even after the Schiff base reaction reached equilibrium. This phenomenon predominantly results from water molecule formation during the reaction, which impedes further progression. Consequently, water-binding agents were introduced to expedite the reaction. In summary, the reaction was executed at a reflux temperature of 81 °C, utilizing a 2:1 molar ratio of 5-chlorosalicylaldehyde to dihydrazide carbonate for 1.5 hours in a laboratory context. This elucidation underscores the criticality of optimizing reaction conditions to maximize efficiency and yield, while simultaneously curtailing costs.

In Figure 2c, the n-π* electron transition within the amine group in the CSHA molecule induces a pronounced absorption peak at a wavelength of 338 nm, as evidenced in the UV curve. Similarly, the π-π* electron transition associated with the benzene ring elicits an absorption peak at 293 nm. Upon comparison with the UV spectra of compounds SSB1 and SSB2, a noticeable red shift in the position of the absorption peak is discerned, as depicted in the figure. This shift can be attributed to the presence of chlorine as an electron-withdrawing group on the benzene ring, which leads to a red shift in the UV spectrum of the compound. Additionally, the amalgamation of the product's infrared spectra corroborated that the synthesized compound possesses the same theoretical structure as CSHA, signifying successful synthesis.

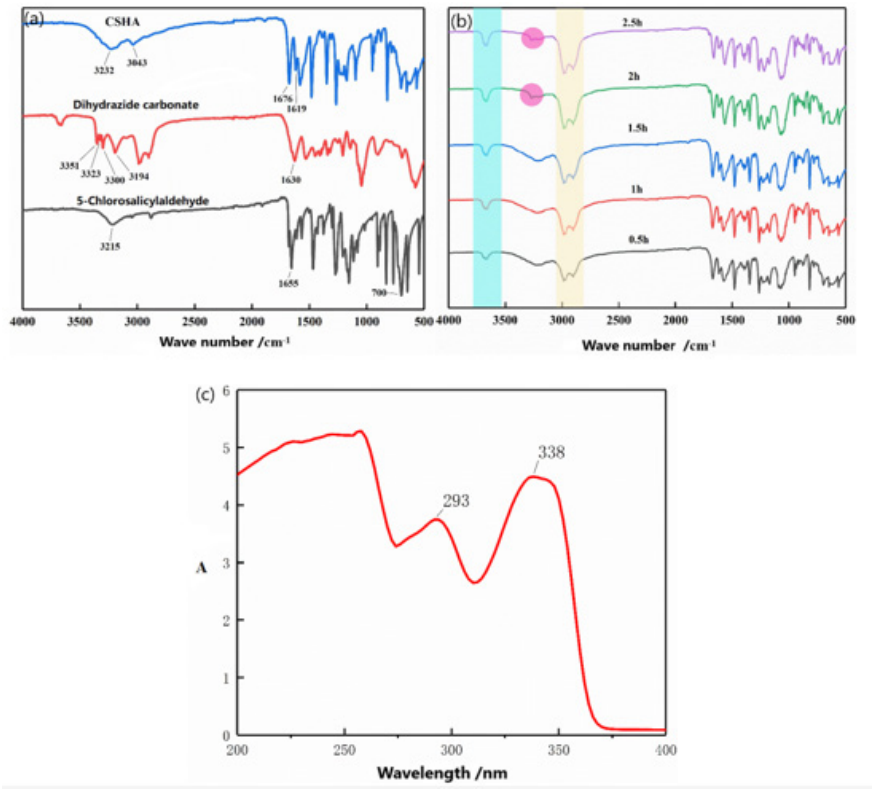

Figure 2: (a) Infrared spectrum of raw material, (b) infrared spectrum of materials at different reaction times, (c) ultraviolet spectrum of CSHA.

Thermal stability analysis

To guarantee the effective and secure dyeing of polyester fabrics with CSHA, meticulous regulation of the process conditions, including temperature and pressure, is imperative. High-temperature and high-pressure dyeing processes are commonly employed for polyester dyeing. Nevertheless, under such stringent conditions, CSHA disperse dyes might undergo decomposition, precipitating side reactions or the deterioration of the imine group in CSHA. Considering the phase transition temperature of CSHA is 172°C and its thermal stability is moderate when contrasted with other disperse dyes [33], the meticulous adjustment of time and temperature parameters during high-temperature and high-pressure dyeing becomes critical. Thermogravimetric analysis (TG) quantifies the sample's weight loss and furnishes visual evidence of thermal stability. Figure 3b and Figure 3c exhibit TG and DTG plots of polyester fabric and CSHA photochromic polyester fabric in N2, with pivotal data delineated in Table 1. The thermal degradation pathway of polyester fabric reveals a singular pyrolysis stage at 350–480°C, culminating in a final carbon residue of 16.33%. Dyeing the polyester fabric with CSHA dye led to a reduction in the initial degradation temperature of polyester T5%, signifying that CSHA dye instigates premature degradation of the matrix during the initial degradation phase. The temperature ascended, reaching the peak thermal decomposition temperature (Tmax) at 420.86°C, whereas the peak thermal decomposition temperature of the dyed polyester fabric was 2.88% higher than that of the original fabric. The ultimate residual carbon was 13.55%, marking a 2.78% reduction compared to the untreated polyester fabric, which implies that CSHA facilitates the carbonization of the polyester fabric. Moreover, the DTG plots reveal that the dyeing with CSHA marginally elevates the weight loss rate of the polyester fabric. These insights underscore the necessity of stringently controlling the dyeing process conditions to assure the effective and secure dyeing of polyester fabrics with CSHA, thereby circumventing potential side reactions or the degradation of the imine group.

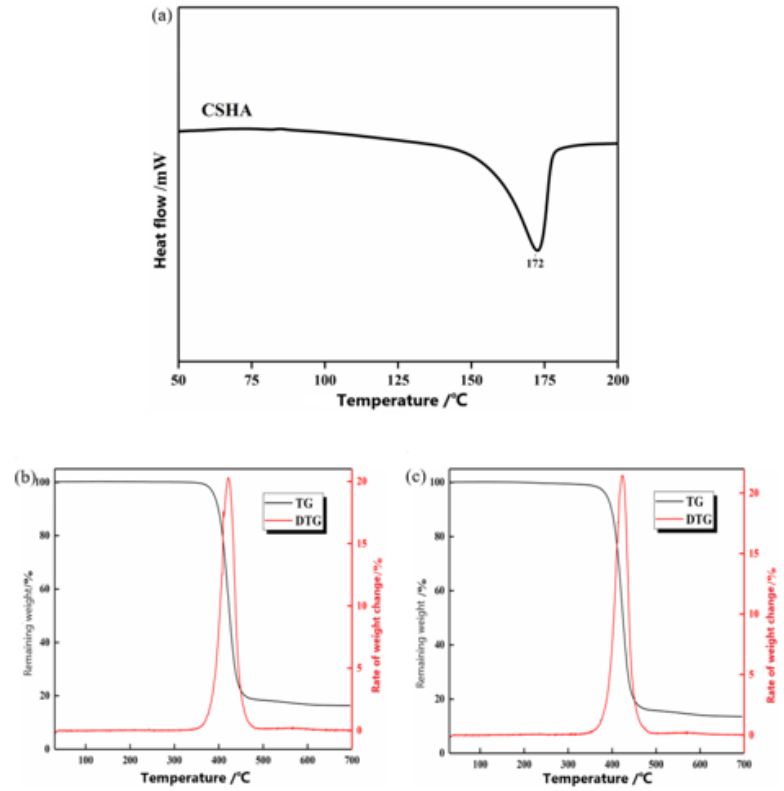

Figure. 3: (a) DSC diagram of CSHA, (b) TG and DTG of original polyester fabric and (c) CSHA photochromic polyester fabric.

Table 1: TG and DTG curve data of polyester fabric and CSHA photochromic polyester fabric.

Samples	$T_{5\%}$	$T_{10\%}$	T_{max}	R_{max}	Residue
	(°C)	(°C)	(°C)	(%/°C)	(%)
Polyester fabric	389.79	398.78	420.86	57.3	16.33
CSHA Photochromic Polyester Fabric	387.84	398.5	423.74	51.72	13.55

Schiff base dye particle size analysis and surface morphology analysis of polyester dyed fabrics

Polyester dyeing processes under high-temperature and high-pressure conditions necessitate specific particle size dimensions for dyes, with disperse dyes commonly utilized for polyester dyeing exhibiting particle sizes beneath 600 nm. Figure 4g illustrates the particle size distribution of CSHA disperse dyes, revealing that, following grinding, ultrasonication, and ball milling dispersion, the particle sizes of CSHA disperse dyes are 296 nm (D50) and 332 nm (D95). Thus, it is evident that the predominant portion of CSHA disperse dyes possesses particle sizes below 332 nm, with the mean particle size being 296 nm. This indicates that CSHA disperse dyes, being nanoscale in dimension, satisfy the particle size criteria for high-temperature and high-pressure dyeing processes.

The images showcased in Figure 4 present the SEM representations of the untreated polyester fabric and the CSHA discolored polyester fabric. The a and b diagrams depict the smooth surface of the initial polyester fabric with spaces between the fibers. Conversely, c and d display the polyester fibers' roughened texture with dye particles adhering to the fiber surface, indicating that the fibers are densely populated with dye particles, albeit of a larger size. This suggests the occurrence of CSHA agglomeration during the dyeing process. The e and f diagrams elucidate that the original cross-section of the polyester fabric is smooth, whereas the cross-section of the CSHA discolored polyester fabric exhibits trace white particles, attributable to the penetration of CSHA dye into the polyester fiber under high-pressure and high-temperature dyeing conditions. Additionally, the electron microscopy analysis confirms the effective penetration and dyeing of the polyester fiber by the CSHA dye. These findings affirm that CSHA dyes are apt for high-temperature and high-pressure dyeing processes of polyester, capable of efficiently diffusing and penetrating the fibers to facilitate a consistent and stable dyeing outcome.

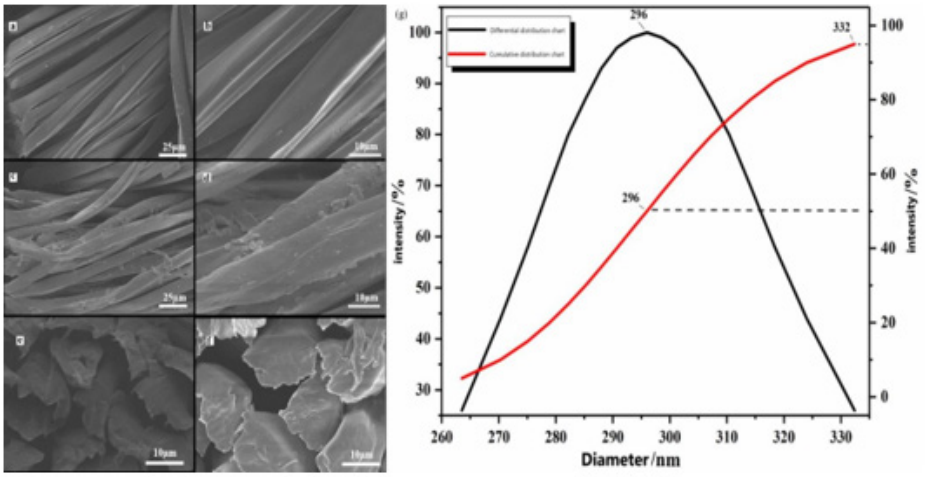

Figure 4: SEM of untreated polyester fabric and CSHA color changing polyester fabric, the original polyester fabric's electron micrographs are shown in (a) and (b) at magnifications of 500 and 2000, respectively; (c), (d) are the electron micrographs of the CSHA polyester discolored fabric at 500x and 2000x, respectively; (e), (f) are the fabric cross-sections of the original polyester fabric and the CSHA polyester discolored fabric at 500x, respectively, (g) particle size distribution of CSHA disperse dyes.

chromatic aberration and dye uptake of CSHA photochromic polyester fabric

Table 2 reveals that with the increment in the o.w.f of the CSHA dye, there is a corresponding increase in the darkness of the polyester fabric over time. Nevertheless, at an o.w.f of 25%, the chromatic aberration attains its peak at of 19.45, which diverges from the expected relationship with brightness. The electron micrograph of the CSHA polyester fabric illustrates that a portion of the CSHA dye adheres to the surface of the polyester fibers. As the o.w.f escalates, a greater quantity of color deposited on the surface, whereas a lesser amount of dye is absorbed inside the fiber. The resultant color of the dyed polyester fabric manifests as a subtly uneven gradient of yellowish-green, which could suggest that some decomposition of CSHA dyes might occur during the dyeing process. Importantly, the exhaustion rate peaked at 33.69% when the o.w.f reached 20%, indicating potential for enhancing the fabric's dyeing efficiency despite the observed progressive increase in exhaustion rate with higher CSHA dye to fabric weight ratios. These insights could illuminate pathways to refine the dyeing process conditions, aiming to augment the dyeing efficiency and secure a consistent and stable dyeing result while circumventing the decomposition of the CSHA dye.

Color-changing property analysis

The CSHA films were fabricated by homogeneously doping 1% CSHA disperse dyes in TPU, and the K/S values of CSHA films were tested under different UV illumination times, as depicted in Figure 5.

Table 2: Effect of CSHA dyes on fabric weight on polyester chromatic aberration and dye uptake.

o.w.f (%)	*DL*	*Da*	*Db*	*DE*	Dye uptake (%)
5	-3.01	-2.35	11.81	12.83	17.32
10	-3.77	-1.68	12.77	13.42	23.64
15	-5.17	-0.2	13.85	14.79	28.14
20	-4.91	-4.93	16.38	16.77	33.69
25	-5.19	-2.32	18.6	19.45	31.32

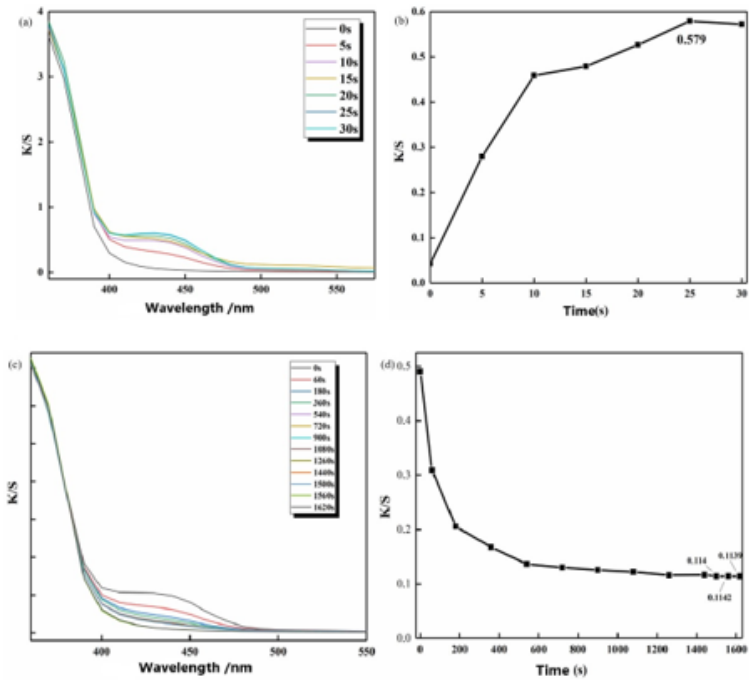

Figure 5: (a) and (b) Variation of K/S value of CSHA photochromic film with UV irradiation time, (c) change of K/S value and (d) time fading of CSHA photochromic film.

Figure 5a presents the K/S curves of CSHA photochromic film at 1% mass concentration subjected to varied durations of UV illumination. Figure 5b depicts the evolution of the K/S value of the CSHA photochromic film at 440 nm subjected to different periods of 365 nm UV light exposure. Examination of Figure 5a reveals that the paramount absorption peak manifests at approximately 440 nm following exposure to 365 nm UV light, culminating in the CSHA film transitioning from colorless to yellow. This transformation suggests an alteration in the molecular structure of CSHA, characterized by proton transfer between the amine and amino groups, the transformation of the alkene amine structure into a secondary amine, and modifications to the molecule's conjugated structure, resulting in a red-shift in the visible absorption spectrum. The data from Figure 5b demonstrates that the K/S value of the CSHA photochromic film at 440 nm exhibits a consistent augmentation with the extension of UV excitation durations. Upon reaching a UV exposure time of 25 seconds, the K/S value peaks at 0.579, beyond which no significant fluctuations in the K/S value of the CSHA photochromic film are observed with further increases in UV irradiation time. This finding suggests that a 25-second UV irradiation period is requisite for the complete color transition of the CSHA photochromic film. Collectively, these results underscore the viability of employing the CSHA photochromic dye in a spectrum of photochromic applications.

Figure 5c illustrates the relationship curve of the K/S value for a 1% mass concentration of CSHA photochromic film under varying UV illumination durations, whereas Figure 5d presents the curve depicting the variation of the K/S value with fading time. Analysis of Figure 5c reveals that the K/S value of the CSHA photochromic film at 440 nm diminishes as the fading time increases, reaching a plateau at 1560 seconds, beyond which the curve remains unchanged. This observation implies that the photochromic film has achieved full

reversion, attributed to the CSHA compound's molecular structure reverting under visible light and dark conditions. Additionally, the proton initially transferred to the imino group gradually returns to the amino group, the conjugation system of CSHA undergoes another transformation, and the color progressively shifts from yellow back to white. Moreover, Figure 5d demonstrates that with an extension of the fading time, the K/S value of the CSHA photochromic film at the wavelength of 440 nm progressively diminishes until it stabilizes at approximately 0.1142, signaling complete reversion. The total fading duration of the CSHA photochromic dye under visible light conditions is 1560 seconds. These results highlight the potential of CSHA photochromic dye for the development of photochromic materials capable of transitioning between two colors upon UV irradiation and subsequently reverting to their original color when exposed to visible light.

Fluorescent properties of CSHA polyester fabrics.

The fluorescence intensity of cotton-printed fabric impregnated with CSHA dye at different on-weight-of-fabric (o.w.f) percentages was quantitatively assessed using a fluorescence spectrophotometer, operating at an excitation wavelength of 365 nm and 400 V; the findings are depicted in Figure 6a. The fabric treated with the fluorescent dye demonstrated an emission peak at approximately 562 nm, corresponding to yellow-green fluorescence, and its fluorescence intensity exhibited a direct correlation with the quantity of dye applied during the printing process. The zenith of fluorescence intensity, quantified at 5207, was attained when the o.w.f percentage of CSHA dyes reached 20%. Beyond this concentration, a plateau in fluorescence intensity was observed, indicating no further increase with increased dye concentration. At an o.w.f percentage of 20%, the fluorescence reflectance of CSHA polyester fabric was recorded at 8.26%, corroborating the observations from the fluorescence reflectance graph of CSHA presented in Figure 6b. These results suggest that the fluorescence intensity on the fabric begins to saturate at this juncture, signifying that the dye has achieved its maximal dye uptake under the specified process conditions. Consequently, CSHA fluorescent dyes demonstrate superior quality, and CSHA polyester fabric exhibits commendable fluorescence performance. These findings hold substantial potential for the innovation of high-quality fluorescence materials applicable across diverse sectors.

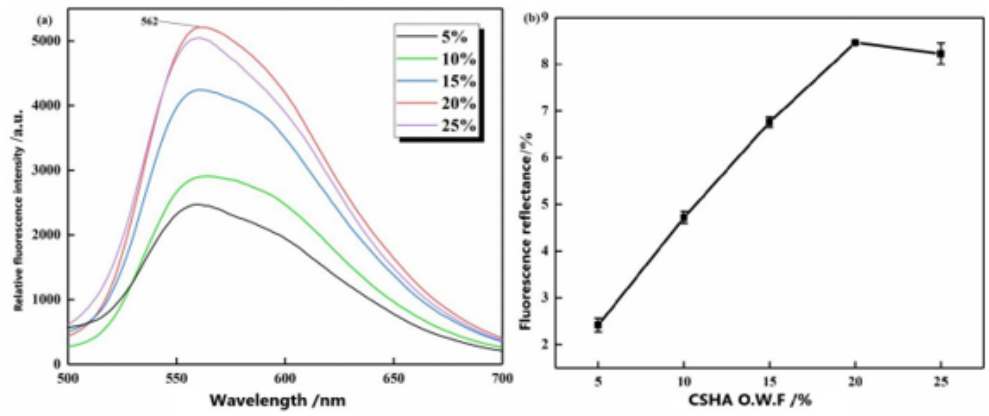

Figure 6: (a) Fluorescence properties of polyester fabrics dyed with different mass fractions of CSHA dyes, (b) relationship between CSHA dyes o.w.f and fluorescence reflectivity of CSHA.

UV resistance of CSHA polyester color change fabric

Schiff base compounds possess the capability to selectively absorb ultraviolet light, attributable to their distinctive intramolecular proton transfer mechanism. The polyester fabric impregnated with CSHA dye exhibits a quantifiable level of ultraviolet radiation resistance.

Figure 7a presents samples A, B, C, D, and E, showcasing the UPF values at 5%, 10%, 15%, 20%, and 25% on-weight-of-fabric (o.w.f) concentrations, respectively. The diagram demonstrates the incremental increase in UPF values correlating with the escalation in o.w.f percentages, with a peak value observed at 15%. With the augmentation of o.w.f percentages and the consequent rise in UPF values, the polyester manifests an emergent anti-UV capability. Accordingly, polyester fabric treated with CSHA dye demonstrates a discernible anti-UV efficacy. Additionally, absorbance and reflectance assays were performed on the relevant polyester fabric to elucidate the anti-UV mechanism of CSHA polyester fabric, as depicted in Figure 7b. Figure 7c reveals that CSHA polyester fabric exhibits certain reflectance and a broad spectrum of UV absorption, with superior absorption of UVB wavelengths compared to UVA. Thus, the anti-UV efficacy of CSHA polyester fabric is attributed to the synergistic effect of UV absorption and reflection. In summation, the analysis of UPF values along with absorbance and reflectance indicates that CSHA polyester fabric possesses inherent anti-UV characteristics, facilitated by the effective synergy between UV absorption and reflection mechanisms. These findings hold significant implications for the application of CSHA polyester fabric in anti-UV endeavors, such as outdoor protective wear and textiles endowed with anti-UV functionality.

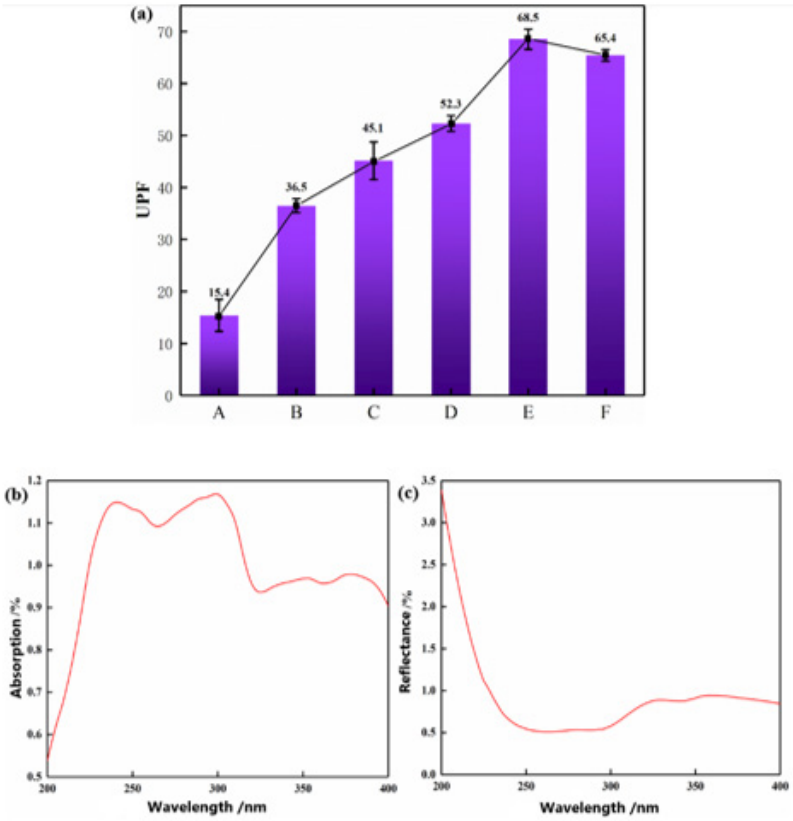

Figure 7: (a) Histogram of UPF value of CSHA compound, (b) absorption and (c) reflectivity of CSHA film.

Analysis of color fastness

Table 3 delineates the color fastness properties of fabrics treated with CSHA dyes at various o.w.f levels. The washing fastness ratings exceed grade 4, while both dry and wet rubbing fastness ratings surpass grade 3. The distinction between dry and wet rubbing fastness is not statistically significant, with CSHA dyes demonstrating moderate sunlight fastness, averaging approximately grade 4. The sublimation fastness, indicative of the stability of disperse dyes within polyester fibers following high-temperature treatments or ironing, is notably deficient for CSHA dyes, achieving only a grade 1-2 as illustrated in Table 3 and the DSC analysis of CSHA. This deficiency is attributed to the phase transition temperature of CSHA, established at 172°C, which signifies the material's limited thermal stability. Upon temperature elevation, the CSHA dyes transition from a solid to a liquid or gaseous state, resulting in the expulsion of the disperse dyes from the polyester fibers and consequently, poor sublimation resistance. In summary, the CSHA disperse dyes exhibit satisfactory color fastness performance, sufficient for standard high-temperature and high-pressure dyeing processes. Nevertheless, the inadequate sublimation fastness restricts their applicability in scenarios involving high-temperature treatments or ironing. These findings have implications for the formulation of novel disperse dyes with enhanced sublimation resistance and color fastness.

Table 3: Color fastness of polyester fabrics treated with different o.w.f CSHA dyes.

Serial number	o.w.f (%)	Washing fastness (grade)	Rubbing fastness (grade)		Sublimation fastness (grade)	Light fastness (grade)
			dry	Wet		
1	5	3-4	4-5	3-4	2	4-5
2	10	4-5	4-5	3	2	4-5
3	15	4-5	3-4	3	2	4
4	20	4	3	3	1	4
5	25	4	3	3	2	4

Conclusion

A novel small molecule compound, 5-chlorosalicylaldehyde carbonyldihydrazide Schiff base (CSHA), was synthesized successfully through the reaction of 5-chlorosalicylaldehyde with carbodihydrazide via ethanol reflux, achieving an 83% yield. The molecular architecture of CSHA was ascertained via infrared and ultraviolet spectroscopic analysis. At room temperature, the compound exhibited a crystalline state, as evidenced by its microscopic morphology. Differential Scanning Calorimetry (DSC) analysis delineated a phase transition temperature for CSHA. The photochromic behavior of CSHA TPU film at a 1% mass concentration was evaluated, revealing that the absorption peak transitioned from the ultraviolet to the visible spectrum pre and post-light exposure. The saturation of CSHA film in terms of the K/S value was attained after 25 seconds of continuous exposure to 365 nm UV light, and the complete reversion time of CSHA under visible light or in darkness was determined to be 1560 seconds. Moreover, when the o.w.f of CSHA disperse dye was set at 20%, the polyester fabric demonstrated optimal fluorescence intensity, characterized by a relative maximum fluorescence intensity and maximum fluorescence reflectance. These outcomes suggest that CSHA possesses superior photochromic, fluorescent, and anti-UV capabilities, rendering it an auspicious material for the creation of advanced photochromic, fluorescent, and anti-UV products, including outdoor protective apparel and textiles.

Jiansheng Dong: Writing - original draft, Methodology, Writing - review & editing, Formal analysis. Wenjun Meng: Visualization, Investigation. Leilei Si: Data curation, Resources. Yudong Wang: Writing Guidelines. Yunjie Yin: Conceptualization, Supervision, Funding acquisition, Project administration.

Conflict of interests

The authors declare that they have no known competing financial interests or personal relationships that could have appeared to influence the work reported in this paper.

Acknowledgements

The authors are grateful for the financial support of Natural Science Foundation of Jiangsu Province (BK2019020945) and Guangxi keypoint research and development program (No. GUIKEAB23075190).

References

1. Chen Z, Liu G, Pu S, Liu SH (2017) Carbazole-based aggregation-induced emission (AIE)-active gold (I) complex: persistent room-temperature phosphorescence, reversible mechanochromism and vapochromism characteristics. Dyes and Pigments 143(1): 409-415.
2. Chen Z, Zhang J, Song M, Yin J, Yu GA, et al. (2015) A novel fluorene-based aggregation-induced emission (AIE)-active gold (I) complex with crystallization-induced emission enhancement (CIEE) and reversible mechanochromism characteristics. Chemical Communications 51(2): 326-329.
3. Chen Z, Liu G, Pu S, Liu SH (2018) Triphenylamine, carbazole or tetraphenylethylene-based gold (I) complexes: tunable solid-state room-temperature phosphorescence and various mechanochromic luminescence characteristics. Dyes and Pigments 159(1): 499-505.
4. Mohammadi A, Yazdanbakhsh MR, Farahnak L (2012) Synthesis and evaluation of changes induced by solvent and substituent in electronic absorption spectra of some azo disperse dyes. Spectrochimica Acta Part A: Molecular and Biomolecular Spectroscopy 89(1): 238-242.
5. Belfield KD, Liu Y, Negres RA, Fan M, Pan G, et al. (2002) Two-photon photochromism of an organic material for holographic recording. Chemistry of materials 14(9): 3663-3667.
6. Pardo R, Zayat M, Levy D, (2011) Photochromic organic–inorganic hybrid materials. Chemical Society Reviews 40(2): 672-687.
7. Washington I,Brooks C, Turro NJ, Nakanishi K (2004) Porphyrins as photosensitizers to enhance night vision. Journal of the American Chemical Society 126(32): 9892-9893.
8. Wei Yb, Tang Q, Gong Cb, Lam MHW (2015) Review of the recent progress in photoresponsive molecularly imprinted polymers containing azobenzene chromophores. Analytica chimica acta 900(2): 10-20.
9. Goulet Hanssens A, Utecht M, Mutruc D, Titov E, Schwarz J, et al. (2017) Electrocatalytic Z→ E isomerization of azobenzenes. Journal of the American Chemical Society 139(1): 335-341.
10. Beharry AA, Woolley GA (2011) Azobenzene photoswitches for biomolecules. Chemical Society Reviews 40(8): 4422-4437.
11. Qian H, Wang YY, Guo DS, Aprahamian I (2017) Controlling the isomerization rate of an azo-BF2 switch using aggregation. Journal of the American Chemical Society 139(3): 1037-1040.
12. Klajn R (2014) Spiropyran-based dynamic materials. Chemical Society Reviews 43(1): 148-184.
13. Lv B, Wu Z, Ji C, Yang W, Yan D, et al. (2015) Spiropyran-induced one-dimensional cyclodextrin microcrystals with light-driven fluorescence change. Journal of Materials Chemistry C 3(33): 8519-8525.
14. Hernández-Melo D, Cervantes R, Tiburcio J (2017) Shuttling Motion in a Host–Guest Complex Triggered by Spiropyran to Merocyanine Reversible Chemical Transformation. The Journal of Organic Chemistry 82(8): 4484-4488.
15. Brügner O, Reichenbach T, Sommer M, Walter M (2017) Substituent correlations characterized by Hammett constants in the spiropyran–merocyanine transition. The Journal of Physical Chemistry A 121(13): 2683-2687.
16. Berkovic G, Krongauz V, Weiss V (2000) Spiropyrans and spirooxazines for memories and switches. Chemical reviews 100(5): 1741-1754.
17. Yokoyama Y (2000) Fulgides for memories and switches. Chemical Reviews 100(5): 1717-1740.
18. Liu XH, Zhao ZX, Zhang W, Yin TT, Zhang HX (2017) Theoretical investigation on the spectroscopic properties of furylfulgide with different substituents and design of novel bis-furylfulgimide photochromes. International Journal of Quantum Chemistry 117(4): e25327-e25330.
19. Heinz B, Malkmus S, Laimgruber S, Dietrich S, Schulz C, et al. (2007) Comparing a photoinduced pericyclic ring opening and closure: Differences in the excited state pathways. Journal of the American Chemical Society 129(27): 8577-8584.
20. Slavov C, Bellakbil N, Wahl J, Mayer K, Rück Braun K, et al. (2015) Ultrafast coherent oscillations reveal a reactive mode in the ring-opening reaction of fulgides. Physical Chemistry Chemical Physics 17(21): 14045-14053.
21. Schönborn JB, Hartke B (2014) Photochemical dynamics of E-methylfurylfulgide—kinematic effects on photorelaxation dynamics of furylfulgides. Physical Chemistry Chemical Physics 16(6): 2483-2490.
22. Wu NMW, Wong HL, Yam VWW (2017) Photochromic benzo [b] phosphole oxide with excellent thermal irreversibility and fatigue resistance in the thin film solid state via direct attachment of dithienyl units to the weakly aromatic heterocycle. Chemical Science 8(2): 1309-1315.

23. Gurke J, Quick M, Ernsting N, Hecht S (2017) Acid-catalysed thermal cycloreversion of a diarylethene: a potential way for triggered release of stored light energy?. Chemical Communications 53(13): 2150-2153.

24. Higashiguchi K, Taira G, Kitai Ji, Hirose T, Matsuda K (2015) Photoinduced macroscopic morphological transformation of an amphiphilic diarylethene assembly: reversible dynamic motion. Journal of the American Chemical Society 137(7): 2722-2729.

25. Amimoto K, Kawato T (2005) Photochromism of organic compounds in the crystal state. Journal of Photochemistry and Photobiology C: Photochemistry Reviews 6(4): 207-226.

26. Bretler S, Bretler U, Margel S (2017) Engineering of new spiropyran photochromic fluorescent polymeric nanoparticles of narrow size distribution by emulsion polymerization process. European Polymer Journal 89(1): 13-22.

27. Nigel Corns S, Partington SM, Towns AD (2009) Industrial organic photochromic dyes. Coloration Technology 125(5): 249-261.

28. Garai B, Mallick A, Banerjee R (2016) Photochromic metal–organic frameworks for inkless and erasable printing. Chemical Science 7(3): 2195-2200.

29. Sameh H, Saemi O, de Alaniz Javier R (2014) Photoswitching Using Visible Light: A New Class of Organic Photochromic Molecules. Journal of the American Chemical Society 136(23): 8169-8172.

30. Qi Q, Li C, Liu X, Jiang S, Xu Z, et al. (2017) A Solid-state photo-induced luminescence switch for advanced anti- counterfeiting and super-resolution imaging applications. Journal of the American Chemical Society 139(45): 16036-16039.

31. Chen L, Xu S, McBranch D, Whitten D (2000) Tuning the properties of conjugated polyelectrolytes through surfactant complexation. Journal of the American Chemical Society 122(38): 9302-9303.

32. Kwok RT, Leung CW, Lam JW, Tang BZ (2015) Biosensing by luminogens with aggregation-induced emission characteristics. Chemical Society Reviews 44(13): 4228-4238.

33. Alghool S, Abd El Halim HF, Dahshan A (2010) Synthesis, spectroscopic thermal and biological activity studies on azo-containing Schiff base dye and its Cobalt (II), Chromium (III) and Strontium (II) complexes. Journal of molecular structure 983(1-3): 32-38.